Electrically controllable surface magnetism on the surface of topological insulator

Jia-Ji Zhu,[1] Dao-Xin Yao,[2] Shou-Cheng Zhang,[3] and Kai Chang[1]

[1]*SKLSM, Institute of Semiconductors, Chinese Academy of Sciences, P. O. Box 912, Beijing 100083, China*
[2]*School of Physics and Engineering, Sun Yat-sen University, Guangzhou 510275, China*
[3]*Department of Physics, Stanford University, CA 94305, USA*

We study theoretically the RKKY interaction between magnetic impurities on the surface of three-dimensional topological insulators, mediated by the helical Dirac electrons. Exact analytical expression shows that the RKKY interaction consists of the Heisenberg-like, Ising-like and DM-like terms. It provides us a new way to control surface magnetism electrically. The gap opened by doped magnetic ions can lead to a short-range Bloembergen-Rowland interaction. The competition among the Heisenberg, Ising and DM terms leads to rich spin configurations and anomalous Hall effect on different lattices.

Introduction.— All-electrical quantum manipulation of the spin degree of freedom of electrons and/or magnetic ions is a central issue in the fields of spintronics and quantum information processing. Spin-orbit interactions in solids is a inherent relativistic effect and can be tuned by an external electric field, i.e., breaking of spatial inversion symmetry. Recent discovery demonstrate that the spin-orbit interactions can invert the conduction and valence bands, and leads to a new state of matter named topological insulator (TI) in a number of materials, such as a two-dimensional (2D) HgTe quantum well [1–3], and three-dimensional (3D) Bi_xSb_{1-x} [4, 5], Bi_2Se_3 and Bi_2Te_3 [6–8]. These TIs possess an insulating bulk and metallic edge or surface states that are protected by the time reversal symmetry (TRS). The energy spectrum of the surface states shows a single massless Dirac cone at Γ point of the Brillouin zone, which was experimentally verified using the angle-resolved photoemission spectroscopy (ARPES) experiments [5, 8, 9]. Electrical tuning of the Fermi energy in 3D TI materials is reported by changing the backgate voltage [10]. Although the energy spectrum of the surface states of 3D TI is very similar with that of graphene, but there is an important difference between graphene and TIs. The helicity of graphene is not defined in regard to the real spin of the electron but to the two sublattices of graphene. Contrastingly, the helicity of the surface state of 3D TI is defined in regard to the electron spin. The helical surface state is spin-momentum locked and certainly leads to spin relevant effects, e.g., spin filtering and giant magnetoresistance, the Ruderman-Kittel-Kasuya-Yosida (RKKY) interaction [11, 12].

The RKKY interaction is an indirect exchange interaction between magnetic ions mediated by itinerant electrons. This long-range spin-spin interaction play a crucial role in magnetic metals and diluted magnetic semiconductor. One can expect that the mediated helical electrons on the surface of a 3D TI must lead to some unusual properties of the RKKY interaction. Importantly, introducing of many magnetic impurities in 3D TIs breaks the TRS and open a gap in the Dirac spectrum of the surface states [13]. This transition makes the massless Dirac electrons become the massive ones and change the spin orientation of the surface states near the Dirac point. The characteristics of the itinerant electron states, e.g., chiral-ity and energy dispersion, determine the spin-spin interaction between magnetic impurities. However, the back action of magnetic impurities also affects the electron states, e.g., the gap opening, and consequently alters the spin-spin interaction. Recent experiments demonstrate that a strong warping effect in the energy spectrum of the surface states of the 3D TIs, e.g., Bi_2Se_3 and Bi_2Te_3 [8, 9, 14]. The warping effect becomes more significant at high Fermi energy, and certainly influences the surface magnetism of 3D TIs.

In this Letter, we draw attention to the surface magnetism of a 3D TI, utilizing the RKKY interaction mediated by helical massless or massive Dirac electrons. From the analytical expression of the RKKY interaction, we demonstrate theoretically that one can implement various quantum spin models by changing applied gate voltage, e.g., the Dzyaloshinskii-Moriya (DM) model, the XXZ model and the XZ model. The gap opening caused by the magnetic impurities results in an additional Ising term in the RKKY interaction and lead to a short-range correlation, i.e., the Bloembergen-Rowland (BR) interaction, when the Fermi energy is located in the gap. The warping effect behaves like an anisotropic momentum-dependent effective magnetic field perpendicular to the surface, leading to an crystallographic orientation-dependent RKKY interaction. The local spins can be arranged in various lattices, e.g., triangular and square lattices formed by the STM technique, the pinning effect, or the Coulomb interaction. The interplay between the unique property of the RKKY interaction and the geometry of spin lattice results in the rich spin configurations of the ground states of spin systems, e.g., the ferromagnetic, antiferromagnetic and spin frustration on the surface of a 3D TI.

Hamiltonian and RKKY interaction.—First we consider two magnetic impurities S_i ($i = 1, 2$) located at R_i mediated by massless Dirac electrons on the surface of 3D TI (see Fig. 1(a)). The Hamiltonian of the system is $H = H_0 + H_i^{int}$, where the massless Dirac electron Hamiltonian [15] $H_0 = \hbar v_F (k_x \sigma_y - k_y \sigma_x) + \frac{\lambda}{2} (k_+^3 + k_-^3) \sigma_z$ and the *s-d* interaction between the magnetic impurities and the electrons $H_i^{int} = -J (\overrightarrow{\sigma} \cdot \mathbf{S}) \delta (\mathbf{r} - \mathbf{R}_i)$. $\mathbf{k}$ is in-plane momentum of electron, $\overrightarrow{\sigma} = (\sigma_x, \sigma_y, \sigma_z)$ is the Pauli matrix denoting real spin of electron. v_F is the Fermi velocity of the surface states, which
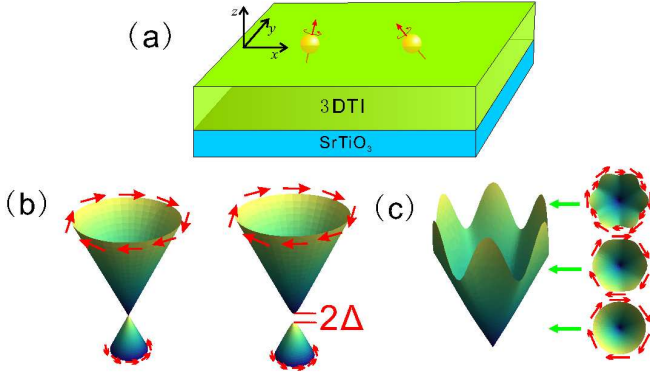
FIG. 1: (color online). (a) Schematic of two local spins on the surface of TI, with electrically controllable RKKY interaction. The 3D topological thin film is epitaxially grown on SrTiO₃ substrates [10]. (b) The massless and massive surface state with spin orientation. The 2Δ denotes the gap caused by breaking TRS. (c) The warping effect of Bi_2X_3 class TI with spin orientation.

is given by $6.2 \times 10^5 \mathrm{ms}^{-1}$ for Bi_2Se_3 [6] and $3.9 \times 10^5 \mathrm{ms}^{-1}$ for Bi_2Te_3 [15]. $\hat{z}$ is a unit vector along the normal direction of the surface. λ is the magnitude of the hexagonal warping term. J denotes the strength of the s-d exchange interaction, which is around $2 \backsim 13$ eVÅ^2 [11].

We first neglect the warping effect, the Green's function in real space can be obtained as $G_\varepsilon(\pm\mathbf{R}) = -\frac{\varepsilon}{4\hbar^2 v_F^2}\left[iH_0^{(1)}\left(\frac{R\varepsilon}{\hbar v_F}\right) \mp \hat{z} \cdot \left(\vec{\sigma} \times \mathbf{n}_R\right) H_1^{(1)}\left(\frac{R\varepsilon}{\hbar v_F}\right)\right]$, where $H_\nu^{(1)}(x)$ is the ν-order Hankel function of the first kind, and $\mathbf{R} \equiv R\mathbf{n}_R$. In the loop approximation we find the RKKY interaction between two magnetic impurities in the form of $H_{1,2}^{RKKY} = -\frac{2}{\pi}\mathrm{Im}\int_{-\infty}^{\varepsilon_F} d\varepsilon \mathrm{Tr}[H_1^{int} G_\varepsilon(\mathbf{R};\varepsilon+i0^+) H_2^{int} G_\varepsilon(-\mathbf{R};\varepsilon+i0^+)]$, where ε_F is the Fermi energy, and Tr means a partial trace over the spin degree of freedom of itinerant Dirac electrons. Then the RKKY interaction can be written as

$$H_{1,2}^{RKKY} = F_1(R,\varepsilon_F)\mathbf{S}_1 \cdot \mathbf{S}_2 + F_2(R,\varepsilon_F)(\mathbf{S}_1 \times \mathbf{S}_2)_y + F_3(R,\varepsilon_F)S_1^y S_2^y, \quad (1)$$

where the range functions are

$$F_1(R,\varepsilon_F) = \frac{J^2}{4\pi^{\frac{3}{2}}\hbar v_F R^3}[G_{2,4}^{2,1}\left(\frac{R^2\varepsilon_F^2}{\hbar^2 v_F^2}\Big|\begin{array}{c}1,2\\\frac{3}{2},\frac{5}{2},0,\frac{1}{2}\end{array}\right) - G_{2,4}^{2,1}\left(\frac{R^2\varepsilon_F^2}{\hbar^2 v_F^2}\Big|\begin{array}{c}1,2\\\frac{3}{2},\frac{3}{2},0,\frac{3}{2}\end{array}\right) + \frac{\sqrt{\pi}}{2}],$$

$$F_2(R,\varepsilon_F) = \frac{J^2}{4\pi^{\frac{3}{2}}\hbar v_F R^3}[G_{2,4}^{2,1}\left(\frac{R^2\varepsilon_F^2}{\hbar^2 v_F^2}\Big|\begin{array}{c}2,\frac{3}{2}\\2,2,0,1\end{array}\right) - G_{1,3}^{2,0}\left(\frac{R^2\varepsilon_F^2}{\hbar^2 v_F^2}\Big|\begin{array}{c}\frac{3}{2}\\1,2,0\end{array}\right)],$$

$$F_3(R,\varepsilon_F) = \frac{J^2}{2\pi^{\frac{3}{2}}\hbar v_F R^3}[G_{2,4}^{2,1}\left(\frac{R^2\varepsilon_F^2}{\hbar^2 v_F^2}\Big|\begin{array}{c}1,2\\\frac{3}{2},\frac{3}{2},0,\frac{3}{2}\end{array}\right) - \frac{3\sqrt{\pi}}{8}].$$

Here $G_{p,q}^{m,n}$ is the Meijer's G-function [16]. The RKKY interaction consists of three terms: the Heisenberg-like term, the DM-like term and the Ising-like term, displaying different range functions. The competition among these three terms can implement various spin models.

All three range functions show damped oscillation as the distance R increases, this behavior indicates that this RKKY interaction is a long-range correlation between two spins (see Fig. 2(a)). Utilizing the asymptotic form of Hankel functions, the long-range asymptotic behavior of the RKKY interaction, i.e., $\varepsilon_F R \gg 1$, is

$$H_{1,2}^{RKKY(asym)} \approx \frac{J^2 \varepsilon_F}{2\pi^2 \hbar^2 v_F^2 R^2}[\sin\left(\frac{2R\varepsilon_F}{\hbar v_F}\right)(\mathbf{S}_1 \cdot \mathbf{S}_2 - S_1^y S_2^y)$$
$$- \cos\left(\frac{2R\varepsilon_F}{\hbar v_F}\right)(\mathbf{S}_1 \times \mathbf{S}_2)_y]. \quad (2)$$

From Eq. (2), the oscillatory behavior of RKKY interaction in a n-type TI ($\varepsilon_F > 0$) can be clearly seen and dominates at large $\varepsilon_F R$. The long-range behaviors of the Heisenberg term and Ising term show a spatial dependence as $1/R^2$, which is the same as in a conventional 2D electron gas, but in contrast with that in graphene where the spatial dependence is $1/R^3$. Interestingly, one can see that the range functions for the Heisenberg and Ising terms have almost the same magnitude but opposite sign. It means that the Ising term always cancel the z-component of the Heisenberg term. By properly adjusting the distance R using the STM technique and/or the Fermi energy ε_F (see Fig. 2(b)), one can even diminish the Heisenberg and Ising terms and obtain a RKKY interaction containing the DM interaction alone. The RKKY interaction becomes $H_{1,2}^{RKKY}(R,\varepsilon_F^c) \simeq F_2(R,\varepsilon_F^c)(\mathbf{S}_1 \times \mathbf{S}_2)_y$, i.e., a pure DM-like spin model. The long-range asymptotic form of the DM interaction also decreases as $1/R^2$, but with $\pm\pi/2$ phase shift compared to other two terms. By setting $\varepsilon_F = 0$, i.e., the intrinsic 3D TI case, the DM term vanishes, the RKKY interaction can be simply written as $H_{1,2}^{RKKY} = \frac{J^2}{16\pi\hbar v_F R^3}\left(2S_1^x S_2^x + 2S_1^z S_2^z - S_1^y S_2^y\right)$, a XXZ-like spin model. Notice that the range function monotonically decreasing as $1/R^3$ (see the inset in Fig. 2(a)) in this case, the same as that in graphene.

The gap opening and warping effects.—Next we study the gap opening effect caused by magnetic impurities in the TIs. The surface states are described by a massive Dirac Hamiltonian $H_0^{(gap)} = \hbar v_F(k_x\sigma_y - k_y\sigma_x) + \Delta\sigma_z$, where 2Δ denotes the gap caused by breaking TRS (see Fig. 1(b)). This Hamiltonian means that the magnetic impurities behave as a Zeeman term which lifts the degeneracy of Dirac point. Similarly, we get the RKKY interaction including the gap opening effect,

$$H_{1,2}^{RKKY(gap)} = F_1^g(R,\varepsilon_F)\mathbf{S}_1 \cdot \mathbf{S}_2 + F_2^g(R,\varepsilon_F)(\mathbf{S}_1 \times \mathbf{S}_2)_y$$
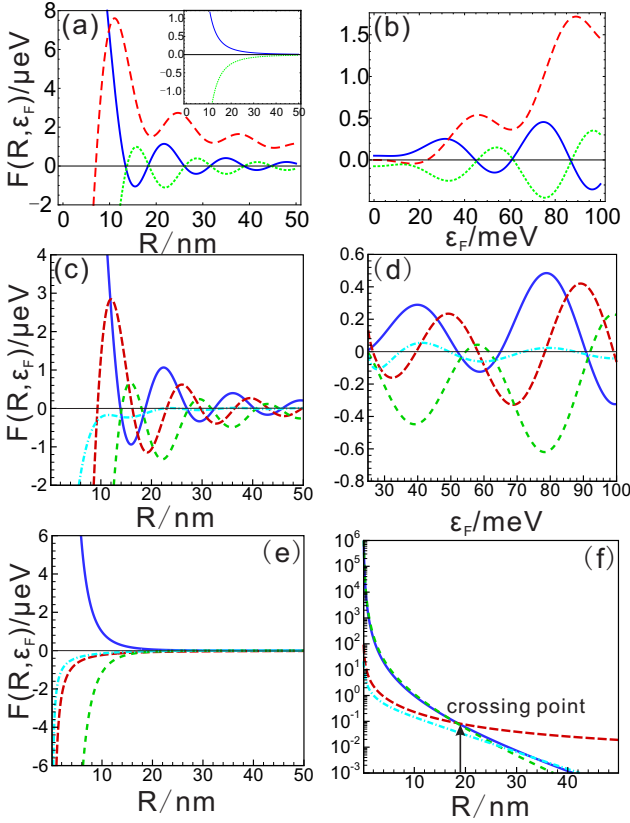$$+ F_3^g(R,\varepsilon_F)S_1^y S_2^y + F_4^g(R,\varepsilon_F)S_1^z S_2^z. \quad (3)$$

FIG. 2: (color online). The range function of RKKY interaction as function of the distance between localized spins R (Fig.2(a,c)) or the Fermi energy ε_F (Fig.2(b,d)). The inset shows the intrinsic case ($\varepsilon_F = 0$). Fig. 2(a),(b) depict the RKKY interaction with massless Dirac electrons, and Fig. 2(c),(d) the RKKY interaction with massive electrons ($\Delta = 25$ meV)[13]. Fig. 2(e) is the range functions of BR interaction, and Fig. 2(f) the absolute values of BR range functions with logarithmic coordinates. The blue (solid) lines are the range function $F_1(R, \varepsilon_F)$, the red (long dashed) lines are the $F_2(R, \varepsilon_F)$, the green (short dashed) ones are $F_3(R, \varepsilon_F)$, and the cyan (dash dotted) ones are $F_4(R, \varepsilon_F)$. We choose $\varepsilon_F = 100$ meV for Fig. 2(a,c), $R = 30$ nm for Fig. 2(b,d) and $\varepsilon_F = -18$ meV for Fig. 2(e,f). The zero point of energy is at the midpoint of the energy gap caused by breaking TRS in Fig. 2(c)-(f).

There are two dominant differences between the RKKY interaction for the gapped (Eq.(3)) and gapless (Eq.(1)) cases when the Fermi energy is located in the conduction band ($\varepsilon_F > \Delta$) (see Fig. 2(c,d)). The first is that the range function of the DM term can be negative for the gapped case. We can still implement the pure DM model by properly choosing a specific Fermi energy ε_F^c and/or the spacing of neighboring spins. The second difference is that the gap opening induces an additional out-of-plane Ising term along the z direction with a relatively weak correlation between the local spins. This is because the gap opening effect looks like a perpendicular magnetic field leading to a Zeeman-like splitting $\Delta\sigma_z$.

When we tune the Fermi energy into the gap, the RKKY interaction can be a short-range interaction, i.e., the BR interaction [17]. Figs 2(e) and 2(f) show that the BR interaction

mediated by massive Dirac electrons also contains all the four terms. This is because the spin orientation on the surface of constant is not influenced by the gap opening away from the vicinity of Dirac point. However, the range functions are totally different. From Fig. 2(e) we can see the Heisenberg term is always antiferromagnetic, while the two Ising terms always give ferromagnetic correlation. Fig. 2(f) shows the exponentially spatial decay behavior of the BR interaction. The Heisenberg term $F_1^g(R, \varepsilon_F)$ and Ising term $F_3^g(R, \varepsilon_F)$ are dominant with almost the same amplitude under a crossing point of spacing $R \simeq 19$ nm, which means one can realize the XZ model $H_{1,2}^{BR} \simeq F_1^g(R, \varepsilon_F)\left(S_1^x S_2^x + S_1^z S_2^z\right)$ on the lattice of the surface of TI. Above this crossing point DM term play the leading role, however, with rather small values.

With increasing the Fermi energy, the warping effect of the energy dispersion of the surface states becomes more significant, resulting in a hexagonal constant energy surface (see Fig. 1(c)). The warping effect behaves like a perpendicular anisotropic effective magnetic field that breaks the rotational symmetry, which is different from the gap opening effect. This anisotropy must lead to an anisotropic, i.e., a crystallographic orientation-dependent RKKY interaction. We consider two local spins arranged along different crystallographic directions (see Table I). These formula indicate that the anisotropic effective magnetic field results in more complicated spin models.

Spin configurations and anomalous Hall effect.—Now we turn to discuss the possible spin configurations of the ground states of the 2D spin systems in the square and triangulated lattices on the surface of 3D TI. The combination of the Heisenberg interaction, DM interaction, and Ising interactions makes it a rich platform to study all kinds of spin configurations. First we consider a pure DM model which can be implemented by tuning the Fermi energy or the spacing of neighboring spins. The DM interaction twist the spin orientation of the neighboring spins and leads to a non-coplanar spin phase or chiral spin phase. For example, the DM interaction cant the spins out of the plane and form an umbrella-like spin structure with a net ferromagnetic moment (see Fig. 3). When chiral electrons hop on the non-coplanar spin sites, the anomalous Hall effect can be realized since they obtain complex phase factor (Berry phase) which works as an internal magnetic field if it is not canceled. Thus the presence of spin chirality and net ferromagnetic moment can yield an anomalous Hall effect on the surface of the 3D TI [18, 19]. In a square spin lattice, the pure DM interaction can lead to a perpendicular nearest neighbor spin ordering. Together with the Heisenberg interaction, the spin ordering can be non-coplanar in the square lattice shown in Fig. 3 (a) . For a triangulated spin lattice, the DM term and ferromagnetic Ising terms can induce spin frustration and have spins to point out of the plane to form a chiral spin state, illustrated in Fig. 3 (b). If we define the spin chirality $\mathbf{S}_1 \cdot (\mathbf{S}_2 \times \mathbf{S}_3)$ to describe the ferromagnetic moment for each triangle, the anomalous Hall effect can happen since the Berry phase is proportional to the spin chirality and may not be canceled [19]. In the Kagome lattice antiferromagnet,

TABLE I: The crystallographic orientation-dependent RKKY interaction caused by the warping effect. The range functions depend on the angle θ which is defined in the direction respect to the [110] crystallographic direction, and are different from the range functions without warping effect.

Crystallographic directions	$H^{RKKY}_{1,2}$
[110]	$F_1^w(R,\theta,\varepsilon_F)\mathbf{S}_1\cdot\mathbf{S}_2 + F_2^w(R,\theta,\varepsilon_F)(\mathbf{S}_1\times\mathbf{S}_2)_y + F_3^w(R,\theta,\varepsilon_F)S_1^y S_2^y + F_4^w(R,\theta,\varepsilon_F)S_1^z S_2^z$
[$\bar{1}$10]	$F_1^w(R,\theta,\varepsilon_F)\mathbf{S}_1\cdot\mathbf{S}_2 + F_2^w(R,\theta,\varepsilon_F)(\mathbf{S}_1\times\mathbf{S}_2)_y + F_3^w(R,\theta,\varepsilon_F)S_1^y S_2^y$
[010]	$F_1^w(R,\theta,\varepsilon_F)\mathbf{S}_1\cdot\mathbf{S}_2 + F_2^w(R,\theta,\varepsilon_F)(\mathbf{S}_1\times\mathbf{S}_2)_z + F_3^w(R,\theta,\varepsilon_F)S_1^y S_2^y + F_4^w(R,\theta,\varepsilon_F)S_1^z S_2^z + F_5^w(R,\theta,\varepsilon_F)S_1^x S_2^x$ $+ F_6^w(R,\theta,\varepsilon_F)\left(S_1^x S_2^y + S_1^y S_2^x\right)$

thermodynamic and neutron scattering measurements have revealed the chiral spin configuration and net ferromagnetism induced by the DM interaction [20]. The anomalous Hall effect can be measured by the transverse Hall conductivity on the surface of 3D TI.
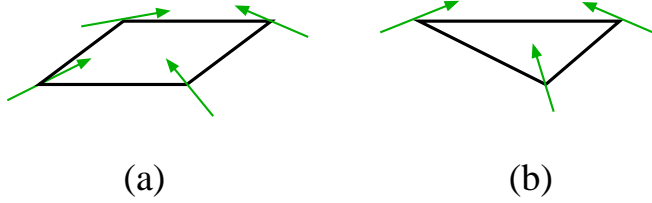

FIG. 3: (color online). Schematic chiral spin configurations of spin systems in the square and triangular lattices with the DM interaction and Heisenberg interaction.

When the antiferromagnetic Heisenberg interaction dominates, the spin configuration is generally collinear or coplanar, which has no spin chirality. The anomalous Hall effect is not expected. The square spin lattice has long-range collinear antiferromagnetic ground state. For a triangulated spin lattice, the long-range coplanar state may develop, like the well known 120° long range order. Since the existence of spin frustration, the ground state of triangulated spin lattices can be highly degenerate and show no long range order. The introduction of DM interaction and ferromagnetic Ising interactions will remove the degeneracy partly or completely. By finely changing the parameters, the spin system can even transit into a spin-glass phase. This means one can construct an artificial spin frustration system utilizing STM technique on the surface of the 3D TI.

Neutron scattering will be a useful tool to detect the surface and bulk spin structure of 3D TI. To enhance the neutron scattering signal from the surface magnetism, it is useful to use large angle neutron scattering technique and pile up many layers of 3D TI with parallel surface.

In summary, we propose a new scheme to manipulate the carrier mediated spin-spin interaction on the surface of the 3D TI electrically, i.e., RKKY interaction and BR interaction. The helical surface state leads to the twisted DM interaction and an in-plane Ising interaction. The gap opening and warping effects introduce isotropic and anisotropic Ising-like terms at low and high Fermi energies, respectively. This spin-spin interaction can be used to realize different spin models by ad-

justing Fermi energy, such as DM model, XXZ model and XZ model. These realizations would not be destroyed by the gap opening caused by the breaking TRS and the warping effect. The surface magnetism of 3D TIs provide us a model platform to study spin configurations and dynamics of various spin models, and pave the way for explore new fundamental physics and new type spintronic devices.

[1] B. A. Bernevig, T. L. Hughes and S. C. Zhang, Science **314**, 1757 (2006).
[2] M. König, S. Wiedmann, C. Brüne, A. Roth, H. Buhmann, L. W. Molenkamp, X. L. Qi and S. C. Zhang, Science **318**, 766 (2003).
[3] J. Li and K. Chang, Appl. Phys. Lett. **95**, 222110 (2009).
[4] L. Fu and C. L. Kane, Phys. Rev. B **76**, 045302 (2007).
[5] D. Hsieh, D. Qian, L. Wray, Y. Xia, Y. S. Hor, R. J. Cava and M. Z. Hasan, Nature **452**, 970 (2008).
[6] H. J. Zhang, C. X. Liu, X. L. Qi, X. Dai, Z. Fang and S. C. Zhang, Nat. Phys. **5**, 438 (2009).
[7] Y. Xia, D. Qian, D. Hsieh, L. Wray, A. Pal, H. Lin, A. Bansil, D. Grauer, Y. S. Hor, R. J. Cava, M. Z. Hasan, Nat. Phys. **5**, 398 (2009).
[8] Y. L. Chen, J. G. Analytis, J. H. Chu, Z. K. Liu, S. K. Mo, X. L. Qi, H. J. Zhang, D. H. Lu, X. Dai, Z. Fang, S. C. Zhang, I. R. Fisher, Z. Hussain and Z. X. Shen, Science **325**, 178 (2009).
[9] D. Hsieh, Y. Xia, D. Qian, L. Wray, J. H. Dil, F. Meier, J. Osterwalder, L. Patthey, J. G. Checkelsky, N. P. Ong, A. V. Fedorov, H. Lin, A. Bansil, D. Grauer, Y. S. Hor, R. J. Cava and M. Z. Hasan, Nature **460**, 1101 (2009).
[10] J. Chen, H. J. Qin, F. Yang, J. Liu, T. Guan, F. M. Qu, G. H. Zhang, J. R. Shi, X. C. Xie, C. L. Yang, K. H. Wu, Y. Q. Li and L. Lu, arXiv:1003.1534.
[11] Q. Liu, C. X. Liu, C. K. Xu, X. L. Qi, and S. C. Zhang, Phys. Rev. Lett. **102**, 156603 (2009).
[12] F. Ye, G. H. Ding, H. Zhai and Z. B. Su, Europhys. Lett. **90**, 47001 (2010).
[13] Y. L. Chen, J.-H. Chu, J. G. Analytis, Z. K. Liu, K. Igarashi, H.-H. Kuo, X. L. Qi, S. K. Mo, R. G. Moore, D. H. Lu, M. Hashimoto, T. Sasagawa, S. C. Zhang, I. R. Fisher, Z. Hussain, Z. X. Shen, Science **329**, 659 (2010).
[14] K. Kuroda, M. Arita, K. Miyamoto, M. Ye, J. Jiang, A. Kimura, E. E. Krasovskii, E.V. Chulkov, H. Iwasawa, T. Okuda, K. Shi-

mada, Y. Ueda, H. Namatame and M. Taniguchi, Phys. Rev. Lett. **105**, 076802 (2010).

[15] L. Fu, Phys. Rev. Lett. **103**, 266801 (2009).

[16] I. S. Gradshteyn and I. M. Ryzhik, *Table of Integrals, Series, and Products (Sixth Edition)*, (Academic Press, New York, 2000), pp. 1022.

[17] N. Bloembergen and T. J. Rowland, Phys. Rev. **97**, 1679 (1955).

[18] X. G. Wen, F. Wilczek and A. Zee, Phys. Rev. B **39**, 11413 (1989).

[19] Y. Taguchi, Y. Oohara, H. Yoshizawa, N. Nagaosa and Y. Tokura, Science **291**, 2573 (2001).

[20] D. Grohol, K. Matan, J.-H Cho, S.-H. Lee, J. W. Lynn, D. G. Nocera and Y. S. Lee, Nat. Mater. **4**, 323 (2005).